Altitude Registration of Limb-Scattered Radiation

Leslie Moy[1], P.K. Bhartia[2], Glen Jaross[2], Robert Loughman[3], Natalya Kramarova[1], Zhong Chen[1], Ghassan Taha[4], Grace Chen[1], and Philippe Xu[5]

[1] Science Systems and Applications, Inc. (SSAI), 10210 Greenbelt Road, Suite 600, Lanham, Maryland 20706 USA
[2] NASA Goddard Space Flight Center, Greenbelt, Maryland, USA
[3] Hampton University, Hampton, Virginia USA
[4] GESTAR, Columbia, MD USA
[5] Science Applications International Corporation (SAIC), Lanham, MD

Correspondence to: Leslie Moy (leslie.moy@ssaihq.com)

Abstract

One of the largest constraints to the retrieval of accurate ozone profiles from UV backscatter limb sounding sensors is altitude registration. Two methods, the Rayleigh Scattering Attitude Sensing (RSAS) and Absolute Radiance Residual Method (ARRM), have been developed to determine the altitude registration to the accuracy necessary for long-term ozone monitoring. The methods compare model calculations of radiances to measured radiances, and are independent of onboard tracking devices. RSAS determines absolute altitude errors, but because the method is susceptible to aerosol interference, it is limited to latitudes and time periods with minimal aerosols. ARRM can be applied across all seasons and altitudes. However, it is only appropriate for relative altitude error estimates. The application of these methods to Ozone Mapping and Profiler Suite (OMPS) Limb Profiler (LP) measurements showed that, at launch, the OMPS LP instrument had a 1-2 km altitude registration error, resulting in a 50% error in the derived ozone density at some altitudes. Though some of the error has been attributed to thermal shifts in the focal plane of the instrument, most of it appears to be due to misalignment of the spacecraft star trackers or the OMPS LP focal plane with respect to the spacecraft axes. In addition, there are ±200 m seasonally varying errors that could either be due to errors in the spacecraft pointing information or in the geopotential height (GPH) data that we use in our analysis.

Keywords: altitude registration, OMPS Limb Profiler, RSAS, ARRM, ozone profile, backscattered ultraviolet

1 Introduction

Instruments that measure the solar radiation scattered by the earth's atmosphere in the limb direction provide a low cost way of measuring stratospheric ozone and aerosol profiles from satellites. The technique provides daily full coverage of the sunlit earth from commonly used polar sun-synchronous satellites. To meet long-term ozone monitoring needs (3% precision between 15 and 50 km) requires the altitude registration of the radiances to be accurate to within ~100 m. For a sensor orbiting at 800 km, this translates into ~6 arcsec accuracy in the pointing direction of the instrument line-of-sight (LOS) with respect to Earth's horizon. This is often a difficult goal to achieve.

In this paper we critically examine the performance of two methods of altitude registration that compare measured and simulated radiances. We discuss the inherent strengths and limitations of each method and then assess their performance using data from the OMPS Limb Profiler (LP), launched onboard the Suomi NPP (SNPP) satellite on October 28, 2011.

One of these techniques, known as Rayleigh Scattering Attitude Sensing (RSAS), is relatively insensitive to instrument radiometric errors and drift. However, since the 350 nm/20 km limb radiances are greatly affected by aerosols, it works best where there is minimal aerosol loading. Under these condistions the accuracy of the method is limited by the accuracy of the geopotential height (GPH) data near 3 hPa (~40 km). Since aerosol contamination limits the range of latitudes and seasons where RSAS can be applied, we developed the Absolute Radiance Residual Method (ARRM). Although ARRM can be applied more broadly than RSAS, it is more suitable to analyzing relative rather than absolute errors in limb altitude registration.

We describe the theoretical basis of these two techniques in Section 2, and move on to results for the OMPS LP instrument in Section 3. Finally, we present several validations of our uncertainty estimates in Section 4.

2 Theoretical Basis

Most scene-based altitude registration methods applied to limb-scattering instruments take advantage of the fact that the atmospheric Rayleigh scattering measured by these instruments varies by 12-14%/km in the absence of particulate scattering by aerosols and clouds and absorption by trace gases. For wavelengths longer than 310 nm, the limb-scattered radiance has a significant contribution from diffuse upwelling radiance (DUR), which is affected by

tropospheric clouds, aerosols and surface albedos from inside a circular cone whose base extends hundreds of km to the horizon. At non-ozone absorbing wavelengths DUR can be as much as half of the measured radiance. Since DUR is challenging to model accurately, all successful altitude registration methods must be relatively insensitive to variations within the cone.

The RSAS method, described in Sect. 2.1, employs signal ratios in which the DUR effects largely cancel. The ARRM, described in Sect. 2.2, uses 295 nm radiances for which ozone absorption screens the DUR signal. The Knee method, described in Sect. 2.3, has been used extensively by others (Sioris et al., 2003; Kaiser et al., 2004; Rault et al., 2005; von Savigny et al., 2005, Taha et al., 2008), but our analysis indicates that it has no advantages over RSAS and ARRM.

2.1 Rayleigh Scattering Attitude Sensor (RSAS)

This technique is named after a sensor that was flown on the Space Shuttle STS-72 in January 1996 (Janz et al., 1996) to test the concept originally proposed by Bhartia in 1992. The technique takes advantage of the fact that the gradient in the log of the limb-scattered (LS) radiance I with altitude z, dlnI/dz, changes by a factor of 3 between 40 km and 20 km for wavelengths near 350 nm (Fig. 1). This is caused by the exponentially increasing attenuation of Rayleigh scattering with pressure. At 40 km this attenuation is small and when aerosol loading is minimal, dlnI/dz is largely determined by dlnP/dz, where P is the atmospheric pressure at altitude z. However, at 20 km the extinction and scattering nearly cancel where the line of sight (LOS) intersects the Earth radius vector at a right angle, called the tangent point (TP). Therefore the radiances at 20 km are relatively insensitive to the exact altitude of the TP. Though several variations of the RSAS technique have been developed (McPeters et al., 2000; Rault et al., 2005; Taha et al., 2008), we find that the simplest formulation described below works as well as any other.

If r is the ratio of radiances for wavelength λ at altitudes z_1 and z_2, and s_1 and s_2 are the vertical slopes dlnI/dz at those altitudes, then the error in tangent height (TH) can be calculated as follows:

$$\Delta z = -\frac{\ln(r)_m - \ln(r)_c}{s(z_1) - s(z_2)} \quad (1)$$

where the subscript m refers to the measured radiance ratios, and c to the ratio calculated using a radiative transfer model. To get the most accurate estimate of TH error the denominator should be as large as possible and the uncertainties in estimating the numerator should be small. The

smallest uncertainties in the numerator occur at wavelengths near 350 nm, where trace gas absorption and aerosol scattering effects are small. Setting z1 to be near 40 km and z2 to be at or below 20 km maximizes the value of the denominator, typically near 0.10/km. So an accuracy of 0.01 (equal to 1% in radiance ratios) is needed to estimate TH within 100 m.

As Fig. 2 shows, the largest source of noise in estimating the numerator comes from the mismatch in cloud sensitivity of radiances at the two altitudes. However, this noise is random and can be reduced by averaging data from multiple orbits.

Aerosols in the instrument's LOS are a more significant source of error. Though the effect of aerosols near 350 nm is small compared to longer wavelengths, it is difficult to model (Fig. 3) due to the determination of subtle differences between two large effects: the reduction of Rayleigh scattering by aerosol extinction and the enhancement of limb radiances by aerosol scattering. In addition, 350 nm LS radiances at 20 km are significantly affected by variation of aerosols along the LOS because of large Rayleigh attenuation; aerosols in the LOS close to the sensor contribute more to the radiance than those far away. Though this effect is similar to the cloud effect mentioned earlier, it is not random because aerosols tend to have systematic latitudinal variability. Given this complexity, the RSAS method works best in latitudes and months where the 350 nm aerosol extinction at 20 km is relatively small.

Another potential source of uncertainty in applying the RSAS technique comes from uncertainty in simulating r_c at 40 km; one needs to have accurate pressure profiles for altitudes at and above 40 km. If the pressure profiles are obtained from geopotential height (GPH) profiles provided by meteorological data assimilation systems, a one-to-one relationship exists between the two errors: a 100 m error in GPH at 3 hPa translates into ~100 m error in determining TH altitude.

2.2 Absolute Radiance Residual Method (ARRM)

This method uses radiances measured by a limb instrument near 295 nm at ~65 km to determine altitude error. The main advantage of ARRM is that it reduces aerosol contamination effects because, with the exception of polar mesospheric clouds (PMCs), the atmosphere is typically free of particulate matter at 65 km. PMCs, which form in the polar summer and are typically located at 80 km, can significantly affect 65 km limb radiances if they are in the LOS of the instrument. Fortunately most of the PMC contamination is screened using a 353 nm channel radiance residual flag at 65 km. Though 295 nm radiances are very ozone sensitive, this

sensitivity drops to less than 0.2% for a 10% change in ozone above 65 km. At this altitude the ozone concentration typically changes by 25% per km, so model radiance errors will be within 0.5% provided the OMPS TH is accurate to 1 km. A second iteration of ARRM will remove any vestige of ozone sensitivity.

The main difficulty in applying ARRM is the inaccuracy of GPH data near 0.1 hPa needed to calculate 295 nm radiances at 65 km. To reduce this error we developed a variation of a technique that has been used for many years to derive mesospheric temperature profiles from the vertical slope of Rayleigh-scattered radiances measured by ground-based UV lidars (McGee et al., 1991). Temperatures were computed using the relative density differences between successive altitudes where the scattering mechanism was purely Rayleigh. Since our technique relies on this region of Rayleigh dominance, their technique can be applied to GPH (which is related to temperature assuming hydrostatic balance). The 350 nm and 295 nm residuals are affected similarly by the errors in the GPH with altitude so we use the 350 nm residual to correct for the GPH errors at 295 nm. Similiarly to the extent that stray light is wavelength independent, this correction will correct for stray light.

The residual at wavelength λ at altitude z, defined as $d(\lambda,z)= \ln I_m(\lambda,z)-\ln I_c(\lambda,z)$, is corrected using 350 nm residuals:

$$d_{corr}(\lambda, z) = d(\lambda, z) - [d(350, z) - d(350, z_0)] \quad (2)$$

where z_0 is a normalization altitude.

The 350 nm differential residuals on the right side of equation (2) provide an estimate of the relative error in calculating radiances using meteorological data between z and z_0. Since this error should be wavelength independent, we can use this term to correct the residuals at any wavelength, assuming that the meteorological data at z_0 is accurate and that the 350 nm wavelength is well calibrated. The large response of OMPS LP at 350 nm results in signals that are the least affected by out-of-band stray light.

The TH error estimated using this method is given by:

$$\Delta z = \frac{d_{corr}(\lambda,z)}{s(\lambda,z)-[s(350,z)-s(350,z_0)]} \quad (3)$$

We are minimizing ozone profile sensitivity by applying this method to radiances at wavelengths shorter than 300 nm. At longer wavelengths DUR makes the LS radiances sensitive to total column ozone at all altitudes. At 295 nm, the use of z near 65 km provides low ozone sensitivity.

Though it is best to set z_0 as low as possible to minimize GPH caused errors, aerosol contamination limits the value to around 40 km.

ARRM has two primary uncertainties. Since 1% error in radiance calibration produces ~70 m error in determining the TH, this method requires accurate radiances (or sun-normalized radiances) and may be affected by instrument degradation. Though the absolute accuracy of ARRM may not be as good as RSAS, this method can be applied at latitudes/seasons where RSAS cannot be applied reliably because of aerosol contamination. And like RSAS, this method is also sensitive to errors in GPH profile near 3 hPa, which are used for calculating 350 nm radiances at 40 km.

2.3 "Knee Method"

The name of this method is derived from the characteristic knee shape of the limb radiance profiles (Fig. 4). Above the knee the radiances decrease with altitude due to exponential decrease in Rayleigh scattering and ozone density. Below the knee ozone absorption becomes so large that it essentially blocks most of the Rayleigh-scattered radiation from reaching the satellite, making the radiances insensitive to atmospheric pressure. This characteristic shape allows estimations of altitude registration error in a manner very similar to that of RSAS. An advantage of this method is the ability to use shorter wavelengths which are less sensitive to aerosols. However, the method requires accurate ozone and pressure profiles near and above the knee region. Radiative transfer calculations using climatological ozone profiles indicate that a 10% error in assumed ozone density (at all altitudes) will produce about a 250 m error in altitude registration (Fig. 5). The method also has a sensitivity to GPH errors that are similar to RSAS and ARRM. In our view this method provides no compelling advantage over comparing the ozone profiles retrieved from a limb scattering sensor with other ozone sensors to determine altitude registration errors. Indeed, direct ozone comparisons are simpler and more reliable if the altitude registration error is the largest error source, and we use this technique to evaluate the results of RSAS and ARRM in Sect. 3.

3 Results

In this section we discuss altitude registration errors in OMPS LP radiances determined first by "Slit Edge" analysis of the instrument focal plane image and then by the application of the RSAS technique. The remaining errors are analyzed using ARRM.

3.1 Slit Edge Results

The OMPS LP sensor utilizes a two-dimensional charge coupled device (CCD) detector to capture spectrally dispersed (along the 740 pixel row dimension) and vertically distributed (along the 340 pixel column dimension) radiation (Fig. 6). Three long vertical entrance slits spaced 4.25° apart produce three distinct images of the atmosphere that are collected simultaneously on the single CCD. The resulting limb radiance profile from the center slit is aligned very closely to the satellite ground track with tangent points trailing approximately 3000 km south of the sub-satellite point. The east and west slit images are separated in longitude by 2.25° (250 km at their tangent points) from that of the center slit.

An unexpected thermal sensitivity was discovered in the LP instrument soon after launch (Jaross et al., 2014). Expansion of the LP instrument's entrance baffle as the sun illuminates it midway through the northern hemisphere causes mirrors in the telescope to rotate slightly, which in turn moves the limb radiance image on the detector. Since there are separate mirrors for each entrance slit, the three slit images move independently. These image motions cause misregistration of both the vertical pointing and center wavelength of each pixel. Vertical pointing changes are detected most clearly by observing the location (detector column) of the lower slit edge, which has a sharp signal gradient. Figure 7 contains plots of the average edge locations in the vertical (altitude) dimension along the orbit. These pointing shifts are very repeatable (ranging only ±15 m at a given point in the orbit over a year).

Since the same slit edge analysis can be applied to pre-launch test data, it is possible to obtain the pixel line of sight shift relative to its calibrated value in the spacecraft reference frame. There is no evidence of image distortion so this shift is the same for all detector pixels within a slit image. The edge analysis indicates the three slit edges shifted by the equivalent of 570/470/950 m (east/center/west slits, respectively) at the middle of an orbit relative to pre-launch measurements. A mean sensor temperature decrease exceeding 25° C from ground to on-orbit conditions is the suspected cause. We believe there are no additional uncorrected pointing shifts arising from

within the LP instrument. An error or change in the alignment of the instrument with respect to S/C axes is not detectable using this method.

Section 3.2 RSAS results

We use the radiative transfer code described by Loughman et al. (2015) to estimate 350 nm radiances. Since the 40/20 km radiance ratio is not sensitive to polarization effects, we use the faster scalar code rather than the full vector one to calculate DUR. The calculations are done assuming a pure Rayleigh atmosphere bounded by a Lambertian reflecting surface at 1013.25 hPa. The reflectivity of this surface is calculated using limb measurements at 40 km. However, both measurements and calculations show that the ratio of 40/20 km radiances is not affected by reflectivity or surface pressure and there is no discernible cloud effect. Since NO_2 only has a very small (<0.5%) effect on 350 nm radiances, climatological NO_2 profiles are sufficient for the calculation. We use OMPS LP retrieved ozone profiles. The RSAS analysis is not sensitive to ozone assumptions because it uses the ozone insensitive 350 nm radiances.

We estimate pressure and temperature versus altitude at the LP measurement locations and time from the Modern-Era Retrospective Analysis for Research and Application (MERRA) data (GEOS-5 FP_IT Np) from the Global Modeling and Assimilation Office (GMAO) at NASA Goddard Space Flight Center (GSFC). The data are provided as geopotential heights (GPH) at 42 pressures from the surface to 0.1 hPa, on a 0.5° latitude x 0.625° longitude horizontal resolution grid, and at a 3 hour interval. The GPH is converted to geometric height using a standard formula that takes into account the variation of gravity with latitude and elevation.

As discussed in Sect. 2.1, RSAS results are affected by aerosols near 20 km. Aerosol profiles derived from the Optical Spectrograph and InfraRed Imaging System (OSIRIS) data (Llewellyn et al, 2004; Bourassa et al, 2007) indicate that tropical aerosols reached a minimum value (during the OMPS lifetime) just before the eruption of the Kelud volcano in Indonesia on February 14, 2014 (Fig. 8). We have therefore chosen to use equatorial RSAS data before the eruption to estimate the altitude registration errors (listed in Table 1). These TH errors range between ~1 and ~1.5 km for the three slits, and have been applied to the Version 2 OMPS LP Ozone data set. Radiative transfer calculations using OSIRIS-derived aerosol profiles indicate that the aerosol caused errors in the results shown are less than 100 m.

Section 3.3 ARRM results

We utilized the same radiative transfer code and profile inputs used for RSAS to calculate radiances at 295 nm. Ozone concentrations from the OMPS LP retrievals were used. As mentioned previously, though 295 nm radiances are very ozone sensitive, this sensitivity drops to less than 0.2% for a 10% change in ozone above 65 km. As discussed in Sect. 2.2, the absolute accuracy of ARRM may not be as good as RSAS, but this method can be applied at latitudes and seasons where RSAS cannot be applied reliably because of aerosol contamination.

Time dependent plots (Fig. 9) show negative pointing trends of approximately 100 m over the four years of data, and even larger seasonal variations depending on the latitude band and slit over the four years of data. Much of this trend is the result of a 6 arcsec (a TH change of ~100m) spacecraft pitch adjustment that occurred on 25 April 2013. Figure 9 clearly shows this abrupt change.

The largest disagreement between the 3 slits (~400 m) occurs in the high northern hemisphere. In the southern hemisphere the disagreement is about 100 m. In addition we see ±200 m seasonally varying errors that could be due to either true pointing changes or errors in the GPH data that we used in our analysis. Such variations in 295 nm radiances cannot be explained by known seasonality in ozone concentration at 65 km.

The ARRM method is designed to accommodate stray light errors that are independent of wavelength. No additional TH errors occur when stray light at 65km is the same at 295 and 350nm. The ground characterization of Limb sensor stray light indicates a small wavelength dependence (Jaross, 2014), and this is removed in ground processing. Our subsequent comparisons with RTM predictions indicate that residual stray light errors at 65 km have a daily mean bias that translates to less than 100 meters in TH.

The ARRM analysis shows a distinct latitude dependence (Fig. 10) with some seasonal differences. While it is tempting to attribute this entirely to TH error, we conservatively do not apply the ARRM results to our data since the uncertainties are of the same magnitude. As with RSAS, this method is sensitive to errors in GPH profile near 3 hPa used for calculating 350 nm radiances at 40 km (see Sect. 4.1). Further analysis is needed to determine the precise cause of the remaining errors.

Section 4 Validation

In this section we consider uncertainties in the parameters used to derive TH errors to indirectly validate the results shown in Sect. 3, and to estimate the remaining uncertainties in the LP TH due to errors in these parameters. Section 4.1 focuses on the validation of 3 hPa GPH information from MERRA that was assumed as the truth in our calculations. In Section 4.2 we consider the reflectivity measured by the OMPS nadir sensor to validate LP-measured radiances at 350 nm, which vary by ~14%/km around 40 km. Finally, in Sect. 4.3 we compare the LP-derived ozone mixing ratio at 3 hPa with the Microwave Limb Sounder (MLS). For the validation studies in this section, the OMPS LP TH has been corrected with the errors listed in Table 1.

Section 4.1 GPH comparison

Errors in the GPH profile assumptions directly translate into TH errors. Although the 3 hPA GPH varies over 4 km along an orbit, a comparison of daily averaged values from MLS and MERRA show differences that are usually less than 200 m (Fig. 11). These differences do not directly explain the latitude dependence of TH errors shown in Fig. 10, but do provide an estimate of the magnitude of errors caused by the use of MERRA GPH in our radiative transfer calculations. There is better agreement at the poles, but this may be due to the reliance on climatology where there are scant measurements. As a result, it is not clear how these GPH errors influence the ARRM results. However, in Section 4.3 we discuss some suggestive but inconclusive results untangling GPH errors from TH errors.

Section 4.2 Radiances comparison

We previously described (in Section 2) the difficulty modeling DUR caused by scene heterogeneity and aerosols. Both the RSAS method and ARRM depend upon an accurate model for DUR at 40 km relative to other altitudes, and any model errors translate directly (Equations 1 and 3) into false estimates in the TH errors.

We estimate the DUR modeling error by comparing LP measurements and modeled 353 nm radiances at 3 hPa. The OMPS Nadir instrument makes nearly simultaneous measurements from a smaller field-of-view (50 x 50 km at nadir).The surface reflectivity derived from its 340 nm

radiances are therefore relatively insensitive to DUR effects (compared to measurements derived from the LP measurements). With better reflectivity assumptions the model/measurement comparisons offer a lower bound of the effect of DUR modeling errors.

The radiance comparison, shown in Fig. 12, suggests model or calibration errors of 2-3% on average, plus structures caused by the limb and nadir scene mismatch. If this error were attributed solely to the limb modeled DUR effect, the resulting TH error would be less than +/- 200 m. There is no evidence of either a seasonal or a latitude dependence in the four days of comparisons, meaning that DUR effects cannot explain the robust seasonal and latitudinal variations seen in ARRM results (Fig. 9 and Fig. 10). These model/measurement comparisons provide an estimate of errors related to incomplete modeling of DUR and inhomogeneous surface albedo included in our RSAS and ARRM results. We therefore conclude those variations arise from errors in the GPH scale or from true TH variations.

Section 4.3 Ozone comparison

At 3 hPa limb ozone retrievals are very sensitive to TH errors, with 20 to 25% per km change in ozone concentration (see Fig. 5). Similar to the Knee Method, we can use this sensitivity to gauge the residual TH errors. We compare LP ozone retrievals against Aura MLS v4 ozone retrievals at 3 hPa (near 40 km) (Fig. 13). While the latitudinal patterns of differences significantly vary with season, we find agreement within ±10% over all seasons and latitude bands. If completely interpreted as due to TH error, a 10% difference would translate to less than 500 m error. These comparisons confirm a residual uncertainty in our scene-based altitude registration techniques of ±200m.

The ARRM method has displayed the ability to track any drifts or sudden changes of 50 m (Sect. 3.3), and time series of TH error derived from the ARRM method track very closely to the time series of the LP/MLS 3 hPa ozone differences (Fig. 14). The highest correlation (0.76) was found at 45° south latitude, with considerable smaller values in the northern hemisphere (0.30 at 60° north). Whether this suggests the ARRM results can be attributed solely to TH errors has not been determined yet.

Both ARRM and LP/MLS ozone comparison depend upon accurate TH and MERRA information, and in the same way. So, while these results suggest some confidence in the ARRM technique, we cannot assign the correlation shown in Fig. 14 to only a TH error or a

MERRA error. It is important to note that MLS ozone profiles are reported as volume mixing ratio on a vertical pressure grid, while the LP algorithm retrieves ozone as number density on an altitude grid. Thus, in order to compare LP and MLS ozone retrievals we had to convert ozone number densities to mixing ratios using MERRA temperature and GPH profiles. This conversion inevitably introduces errors in MERRA GPH and temperature into the ozone comparisons. Therefore ozone differences between LP and MLS ozone retrievals not only depend on the LP TH error, but on errors in MERRA GPH as well as on errors in the retrieval algorithms and instrumental sampling (geophysical noise). Furthermore, analysis of LP and MLS ozone retrievals indicates a large daily ozone variability within a 5-degree latitude bin at 3 hPa that ranges from 2% in the tropics to 20% at high latitudes with the seasonal maximum during austral winters (results are not shown here), which can give readers a sense of geophysical ozone variability. In consideration of all of the above factors, we remain cautious in making definite conclusions and applying time-dependent corrections for the LP TH at this time; further analysis and comparisons with independent ozone observations (like SAGE III) are needed to confirm the results.

Section 5 Conclusions

Accurate altitude registration is key to the success of the limb scattering measurement technique. We have described two scene-based techniques that together provide highly precise and accurate estimates of the tangent height. These altitude registration techniques are inexpensive and more comprehensive than external sources of altitude information, such as star trackers mounted on the spacecraft. Star trackers are typically used on spacecraft when accurate pointing knowledge is desired, but this accuracy does not necessarily transfer to the limb measurements. In Section 3.1 we've described pointing shifts that occur within the sensor optics. Though we were able to calibrate thermal sensitivities within the OMPS instrument, we have yet to identify the source of 1-1.5 km pointing errors derived from RSAS (see Table 1). These may arise from mounting offsets of the instrument and star trackers, or from spacecraft flexure between the two.

The RSAS and ARRM techniques are complementary because the former is accurate to ±200 m, but only under limited conditions. The accuracy of ARRM cannot be easily established, but it has a precision within

±200 m. We believe this results in small, less than 100 m, trend uncertainties for sufficiently long time series, as demonstrated by the OMPS ARRM record.

The single largest source of uncertainty in both techniques is knowledge of the vertical profiles of pressure, which must be provided from external sources. Given uncertainties in GPH data, as seen in the MLS comparison, as well as uncertainties in our ozone retrieval algorithm (not related to TH error), it is currently not possible to tell if the latitudinal and seasonal variations seen in ARRM results are caused by TH error. Further work will be needed to understand their cause. We have shown, however, that ARRM is capable of deriving multi-year trend uncertainties that are on the order of 100m or smaller. Furthermore, the two TH registration methods discussed in the paper allow us to track any drifts or sudden changes in our altitude registration to better than 50 m, which is the minimum level necessary to derive accurate ozone trends from a limb technique.

Acknowledgements: The authors gratefully acknowledge the assistance of NASA's Limb Processing Team in providing the data used in this paper. We would also like to thank Dave Flittner, Ernest Nyaku and Didier Rault, helped with the development and updates of the RT model. Finally, we'd like to acknowledge the role Didier played in laying the groundwork for the OMPS limb retrieval algorithm

References

Bourassa, A. E., Degenstein, D. A., Gattinger, R. L., and Llewellyn, E. J.: Stratospheric aerosol retrieval with optical spectrograph and infrared imaging system limb scatter measurements, J. Geo-phys. Res., 112, D10217, doi:10.1029/2006JD008079, 2007.

Jaross, G., P. K. Bhartia, G. Chen, M. Kowitt, M. Haken, Z. Chen, P. Xu, J. Warner, and T. Kelly: OMPS Limb Profiler instrument performance assessment, J. Geophys. Res. Atmos., 119, doi:10.1002/2013JD020482, 2014.

Janz, S. J., E. Hilsenrath, D. E. Flittner, and D. F. Heath, Rayleigh scattering attitude sensor, Proc. SPIE 2831, Atmospheric Ultraviolet and Space Remote Sensing: Methods and Instrumentation, 146, doi:10.1117/12.257207, 1996.

Kaiser, J. W., C. Von Savigny, K.-U. Eichmann, S. Noel, H. Bovensmann, and J. P. Burrows, Satellite-pointing retrieval from atmospheric limb-scattering of solar UV-B radiation, Can. J. Phys., 82, 1041-1052, 2004.

Llewellyn, E. J., N. D. Lloyd, D. A. Degenstein, R. L. Gattinger, S. V. Petelina, A. E. Bourassa, J. T. Wiensz, E. V. Ivanov, I. C. McDade, B. H. Solheim, J. C. McConnell, C. S. Haley, C. von Savigny, C. E. Sioris, C. A. McLinden, E. Griffioen, J. Kaminski, W. F. Evans, E. Puckrin, K. Strong, V. Wehrle, R. H. Hum, D. J.W. Kendall, J. Matsushita, D. P. Murtagh, S. Brohede, J. Stegman, G. Witt, G. Barnes, W. F. Payne, L. Piche, K. Smith, G. Warshaw, D. L. Deslauniers, P. Marc-hand, E. H. Richardson, R. A. King, I. Wevers, W. McCreath, E. Kyrölä, L. Oikarinen, G. W. Leppelmeier, H. Auvinen, G. Megie, A. Hauchecorne, F. Lefevre, J. de La Noe, P. Ricaud, U. Frisk, F. Sjoberg, F. von Scheele, and L. Nordh: The OSIRIS instrument on the Odin spacecraft, Can. J. Phys., 82, 411–422, 2004.

Loughman, R., D. Flittner, E. Nyaku, and P. K. Bhartia, Gauss–Seidel limb scattering (GSLS) radiative transfer model development in support of the Ozone Mapping and Profiler Suite (OMPS) limb profiler mission, Atmos. Chem. Phys., 15, 3007-3020, 2015.

McGee, T. J., D. Whiteman, R. Ferrare, J. J. Butler, and J. Burris, STROZ LITE: Stratospheric ozone lidar trailer experiment, Opt. Eng., 30, 31-39 (1991).

McPeters, R. D., S. J. Janz, E. Hilsenrath, T. L. Brown, D. E. Flittner, and D. F. Heath, The retrieval of O3 profiles from limb scatter measurements: Results from the Shuttle Ozone Limb Sounding Experiment, Geophys. Res. Lett., 27, 2597-2600, 2000.

Rault, D.F., Ozone profile retrieval from Stratospheric Aerosol and Gas Experiment (SAGE III) limb scatter measurements, J. Geophy. Res., 110, D09309, doi:10.1029/2004JD004970, 2005.

Sioris, C. E., et al., Stratospheric profiles of nitrogen dioxide observed by Optical Spectrograph and Infrared Imager System on the Odin satellite, J. Geophys. Res., 108(D7), 4215, doi:10.1029/2002JD002672, 2003.

Taha, G., G. Jaross, D. Fussen, F. Vanhellemont, E. Kyrölä, and R. D. McPeters, Ozone profile retrieval from GOMOS limb scattering measurements, J. Geophys. Res., 113, D23307, doi:10.1029/2007JD009409, 2008.

von Savigny, C., J. W. Kaiser, H. Bovensmann, J. P. Burrows, I. S. McDermid, and T. Leblanc (2005), Spatial and temporal characterization of SCIAMACHY limb pointing errors during the first three years of the mission, Atmos. Chem. Phys., 5, 2593-2602, doi:10.5194/acp-5-2593-2005.

Table 1: RSAS results at the equator before the Kelud eruption 2014 February. The time period had a minimum value (during OMPS life time) and was chosen using OSIRIS measurements (Fig.8).

TH error, km	**EAST**	**CENTER**	**WEST**
RSAS results	1.12	1.37	1.52

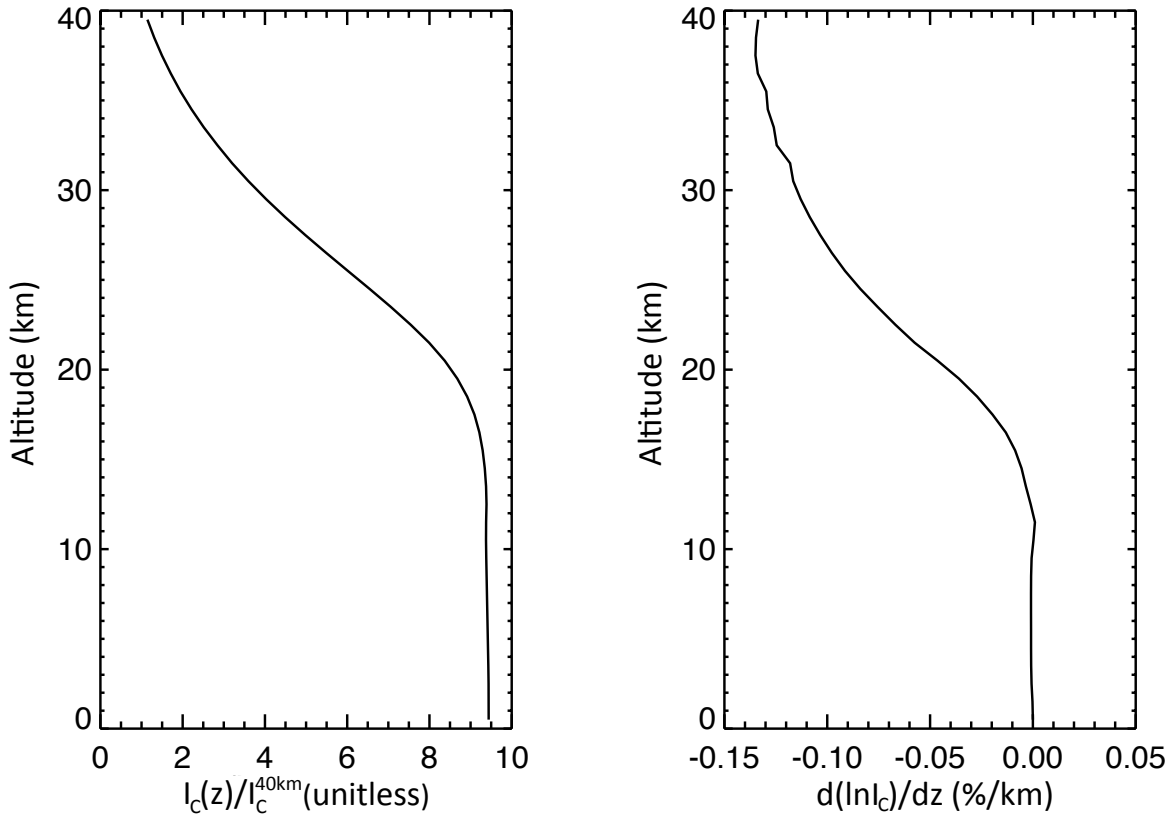

Figure 1: Figure 1a shows calculated 350 nm radiances as a function of altitude, normalized at 40.5km. The calculation models the OMPS LP field of view without aerosols. The shape of the curve originates from the competition between molecular scattering, which increases roughly linearly with pressure, and attenuation which becomes important when the Rayleigh optical thicknesses near the tangent point start to become large. Attenuation causes the slope of 350 nm radiances to change sharply between 40 and 20 km (Fig. 1b), a ~9% /km difference between 20 and 40 km. The slope is used to estimate altitude registration errors by comparing measured ratios with model simulated ratios.

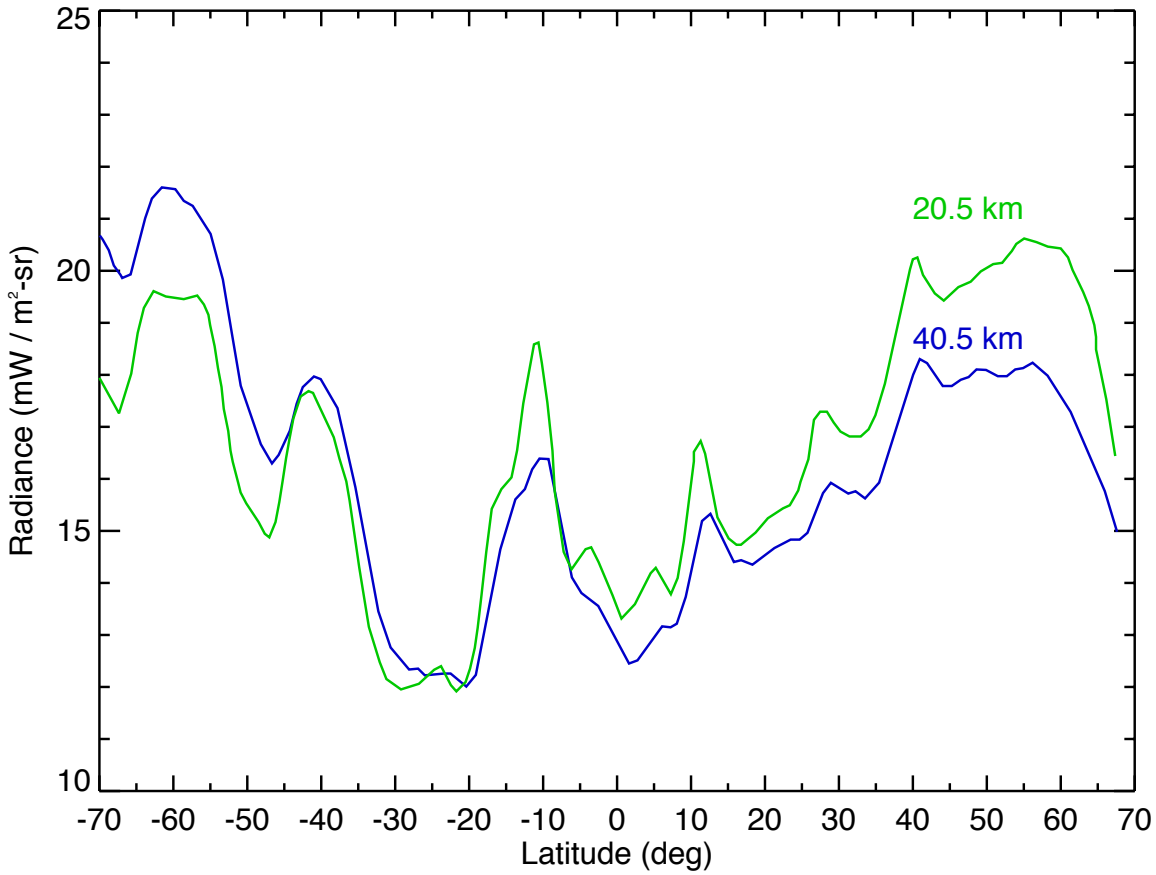

Figure 2: The 353 nm sun-normalized radiances from one orbit of OMPS LP (central slit) taken on Feb. 2, 2012. The blue line shows 40.5 km values and the green line shows 20.5 km values (divided by 8 to put both curves on a similar scale) versus latitude. Since the global aerosol loading on this day was small, the short scale features in both curves are largely caused by variations in cloud and surface albedo. The 20.5 km curve has sharper features and appears to be shifted towards toward the South Pole. This is because large Rayleigh attenuation at 20.5 km causes the radiances to have much higher sensitivity to the atmosphere on the satellite side of the tangent point (TP), while 40.5 km radiances have similar sensitivities to both sides. This effect creates large noise in applying the RSAS technique to orbital data. However, since the noise varies randomly from orbit to orbit, it can be reduced by averaging data from multiple orbits. Figure 6 of Loughman et al. (2015) is an example of how the contributions become asymmetric about the tangent point at lower THs.

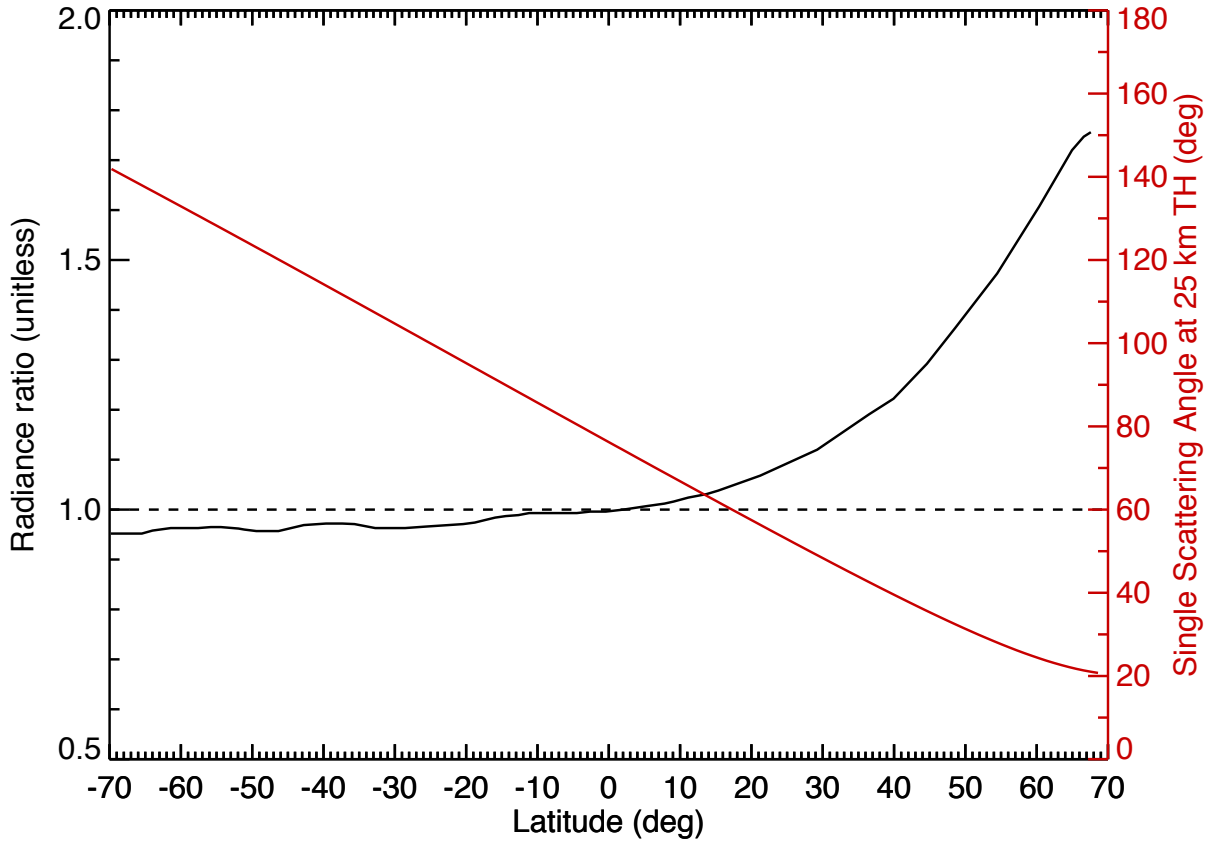

Figure 3: The ratio of 353 nm limb-scattered radiances at 20.5 km with and without aerosols (left axis) and single scattering angle (right axis) as a function of latitude. A nominal latitude-independent aerosol extinction profile was used in the calculation for the OMPS LP viewing geometry on Feb 2, 2012. The strong latitude dependence is caused by an order of magnitude change in aerosol scattering phase function with latitude combined with the attenuation of Rayleigh-scattered radiation by aerosols along the line-of-sight (LOS). In the southern hemisphere, where LP measures aerosols in the backscatter direction, the latter effect dominates and the radiation decreases. The net effect is very sensitive to altitude, variation of aerosol extinction profile along the LOS, and aerosol particle size distribution, and is therefore difficult to calculate accurately.

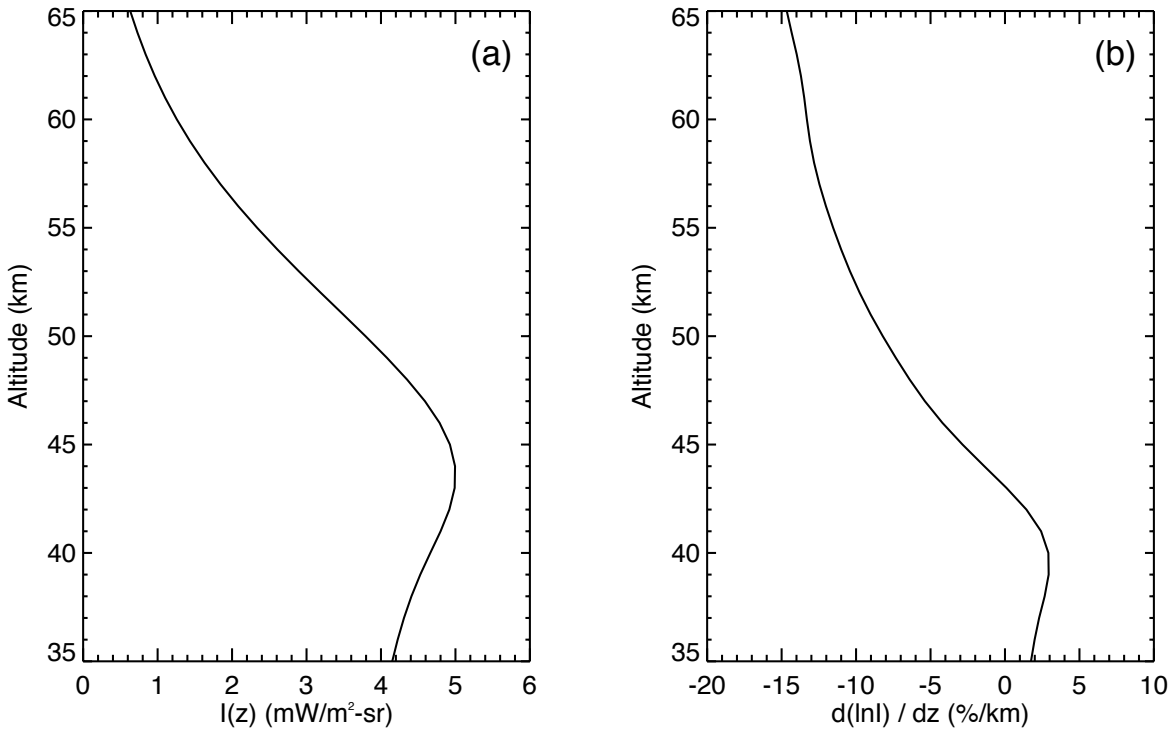

Figure 4: Figure 4a shows calculated 305 nm radiances as a function of altitude assuming an atmosphere with no aerosols. The slope (Fig. 4b) is caused by competition between Rayleigh scattering and ozone absorption near the altitude of maximum radiance, ~44 km. Above 55 km the sensitivity is nearly constant in height, ~13%/km at 65 km. Above the knee the radiances decrease with altitude due to the exponential decrease in Rayleigh scattering and ozone density. Below the knee the ozone absorption becomes so large that it essentially blocks most of the Rayleigh-scattered radiation from reaching the satellite, making the radiances insensitive to atmospheric pressure. This characteristic knee shape allows one to estimate altitude registration error in a manner very similar to that of RSAS, but also makes it is very susceptible to ozone profile assumptions, as illustrated in Fig. 5.

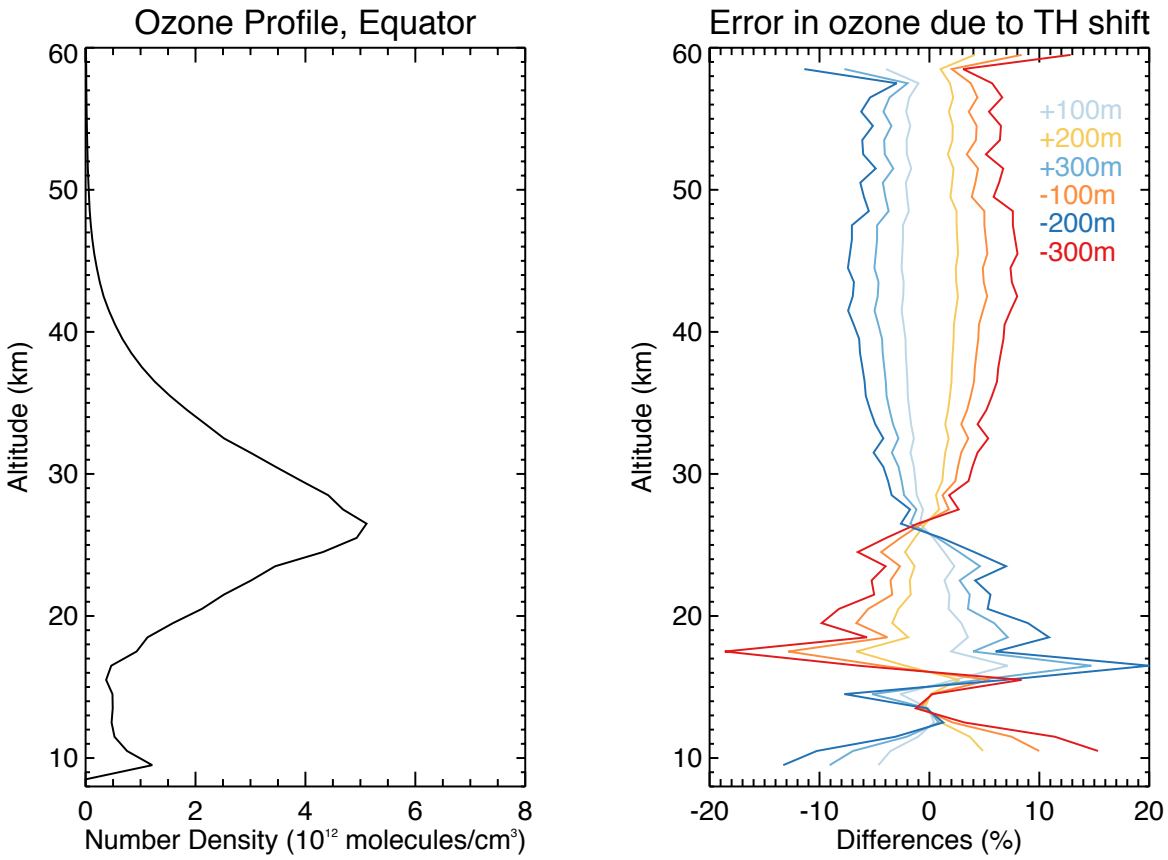

536
537 **Figure 5:** Typical ozone profile in the tropics (such as the one shown in the left panel) peak
538 between 25 and 30 km. By shifting the ozone profile we can estimate an order and pattern of
539 error in ozone profiles due to TH shift (right panel). Errors in ozone retrievals are within 8% at
540 40 km from TH errors of 300 m. Errors are least sensitive at the ozone peak, and are more
541 variable below.
542

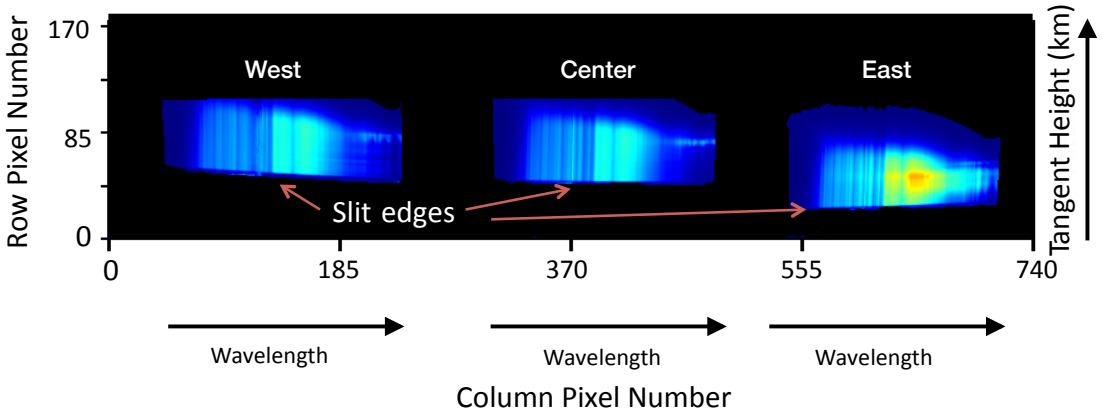

Figure 6: OMPS LP CCD high gain earth viewing radiance images for the three slits (east/center/west). The east and west slit images are separated in longitude by 2.25° from that of the center slit. The wavelength range for each image is 270 to 1050 nm and the minimal TH range is 0 to 80 km. The CCD has 740 pixels in the wavelength dimension. There are 340 pixels in the spatial dimension; the high gain images occupy the lower half of the CCD (pixels 0 to 170). The spatial extent of each slit's image on the detector is limited by the vertical length of that slit. The lower slit edges (nearest the Earth surface) provide a high contrast signal cutoff that can be monitored for movement.

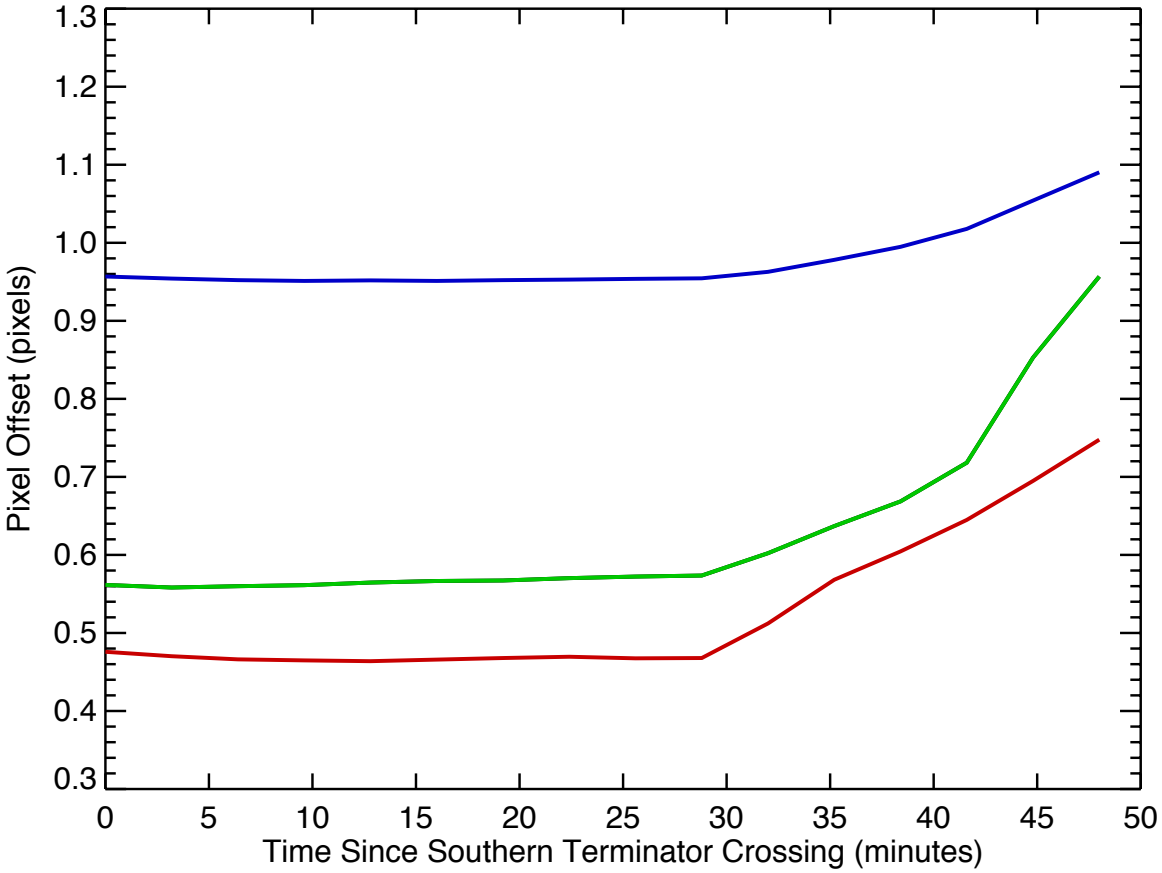

Figure 7: Slit edge results for the three slits (Green=East Slit, Red=Center Slit, Blue=West Slit) plotted against time since Southern Terminator crossing. A 1 pixel shift corresponds to a 965 m TH shift. The offsets are stable from the southern terminator to the mid latitude northern hemisphere where the exposure to the sun increases thermal effects.

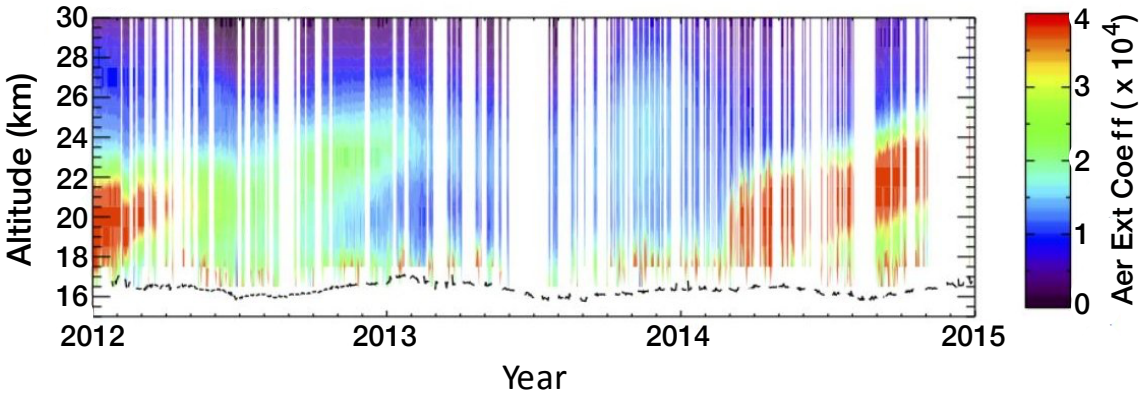

559

560 **Figure 8:** Time series of OSIRIS aerosol extinction profiles above the tropopause (dashed line).
561 The large concentration in 2012 is due to the June 2011 Nabro eruption in Eritrea. The aerosols
562 at 20 km reached a minimum value (during OMPS life time) just before the eruption of the
563 Kelud Volcano on 14 February 2014.

564

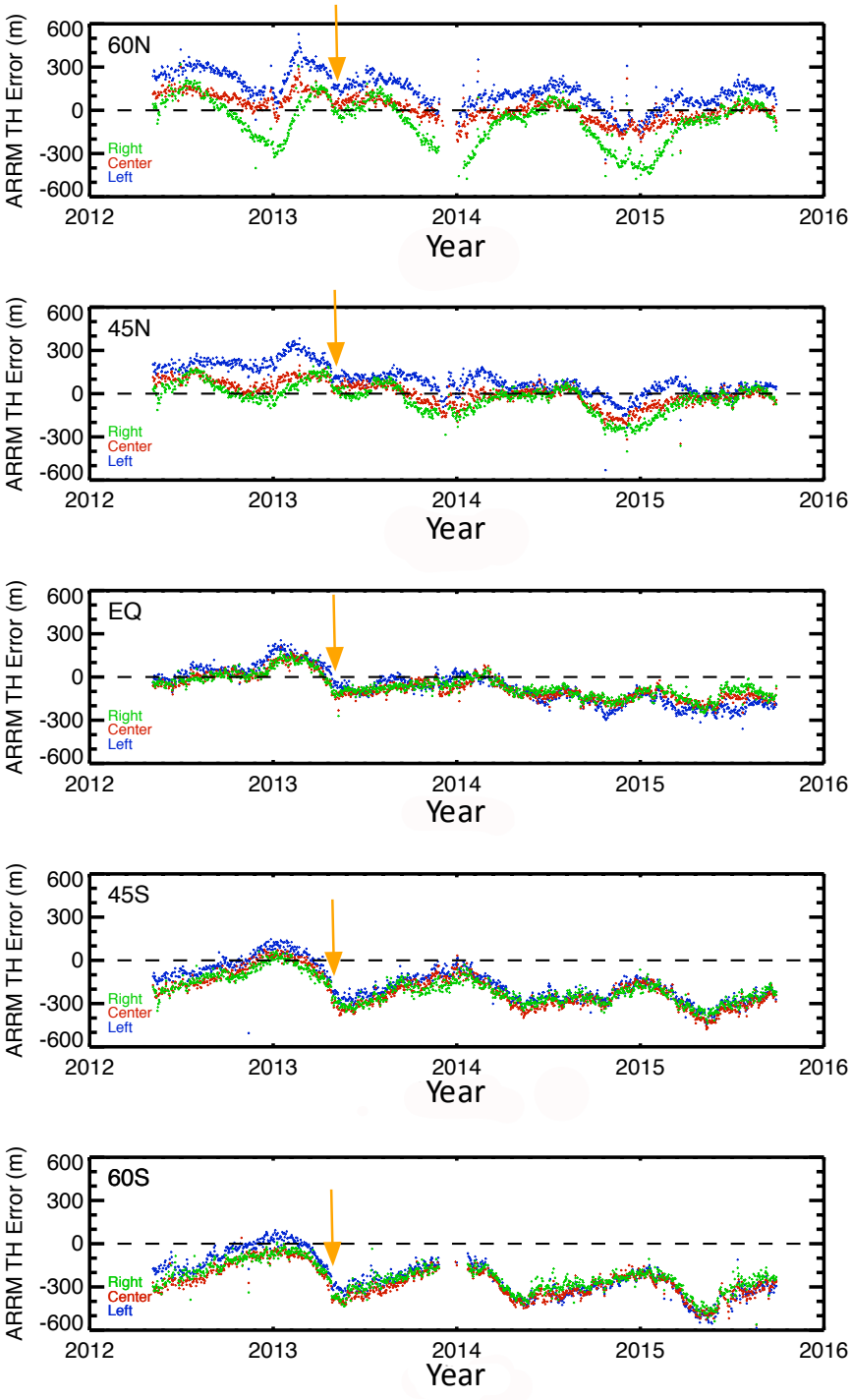

Figure 9: Time dependent plots of TH errors from ARRM analysis at five latitude bands for the three slits. Values are normalized at the Equator just prior to the Kelud eruption on February 14, 2014 based on the RSAS results summarized in Table 1. Arrows indicate a 12 arcsec pointing adjustment to one of the two spacecraft star trackers on April 25, 2013. The resulting 100 m TH shift can be seen most clearly by comparing 2012 and 2013 results. Slit discrepancies and seasonal dependencies of +/-200 m can also be seen.

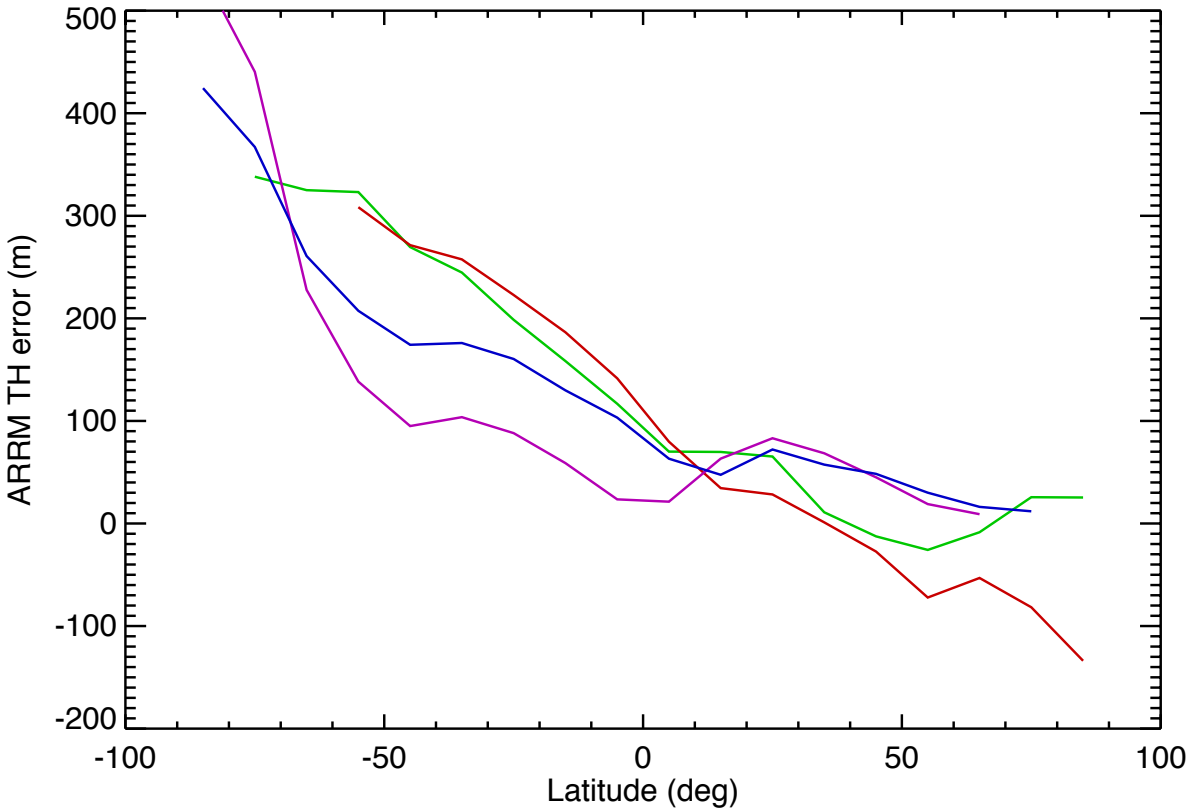

572
573 **Figure 10:** Average (over the ~4 year study period) ARRM results by latitude and seasons
574 (MAM-green, JJA-red, SON-purple, DJF-blue) for Center Slit. Excluding the extreme polar
575 regions, there appears to be an average 300 m TH change over an orbit.
576

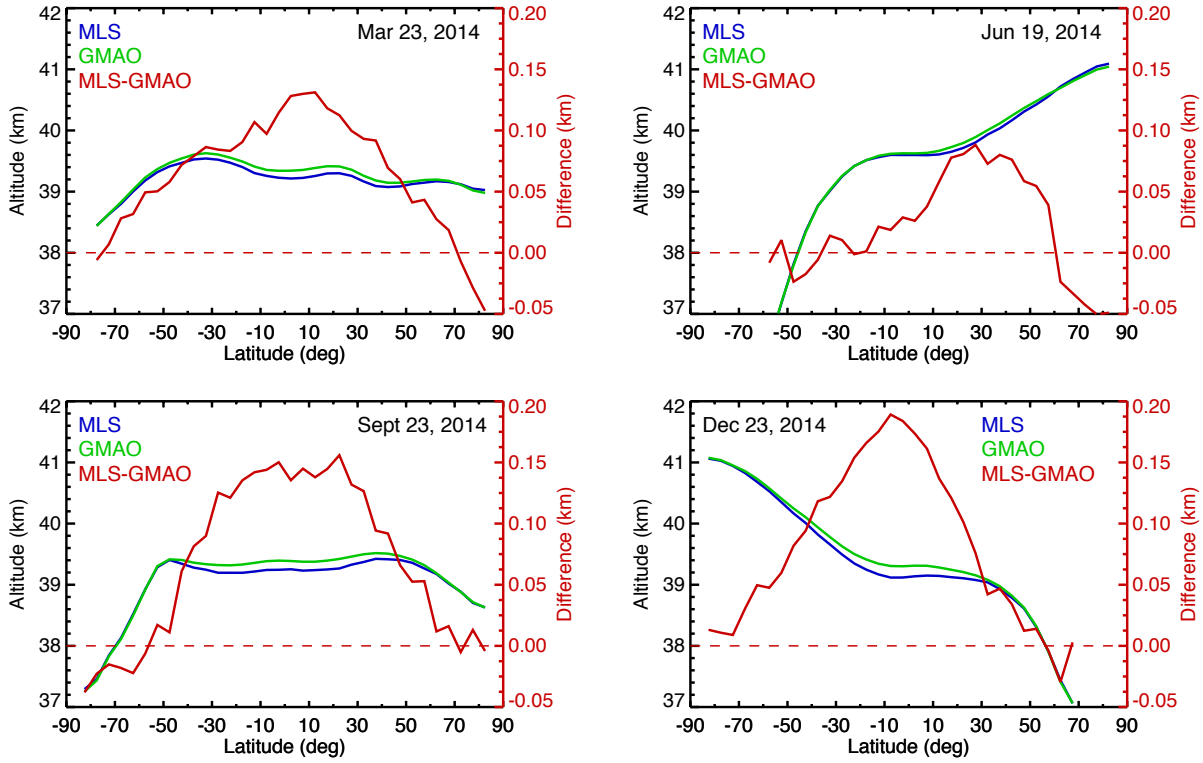

Figure 11: Daily five degree zonal means of GPH from MLS (blue), GMAO (green), and the difference MLS-GMAO (red) at 3 hPa GPH for four cardinal days. Note that despite a 2 to 4 km change over an orbit, the differences are generally within 200 m. These differences provide an estimate of the errors caused by the use of MERRA GPH in our radiative transfer calculations. Better agreement seen at the poles may simply be due to the fact that there are not many measurements at these latitudes and both may be influenced by the same climatology. If this error were attributed solely to the limb model and only at one altitude, the resulting TH error would be less than +/-200 m. There is no evidence of either seasonal or latitude dependence in the comparison, meaning that DUR effects cannot explain the variations seen in Fig. 9.

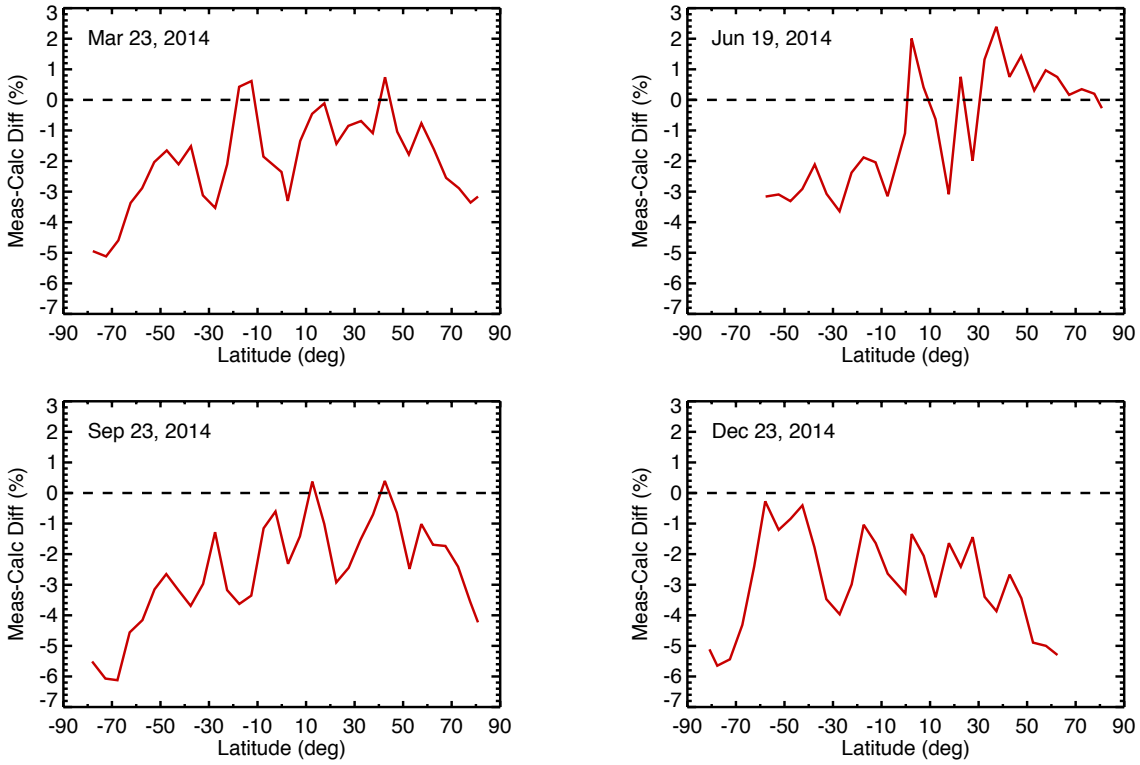

588
589 **Figure 12:** We have estimated the DUR modeling error by comparing 353 nm measured and
590 modeled radiances at 3 hPa. The radiances are modeled using an independent, nearly
591 simultaneous measure of surface reflectivity derived from the OMPS Nadir instrument at 340
592 nm. The 50x50 km nadir-view measurements are relatively insensitive to DUR effects. The
593 radiance differences (given for the same four cardinal days as in Fig. 11) suggest model or
594 calibration errors of 2-3% on average, plus structure caused by the contributing limb and nadir
595 scene mismatch.
596

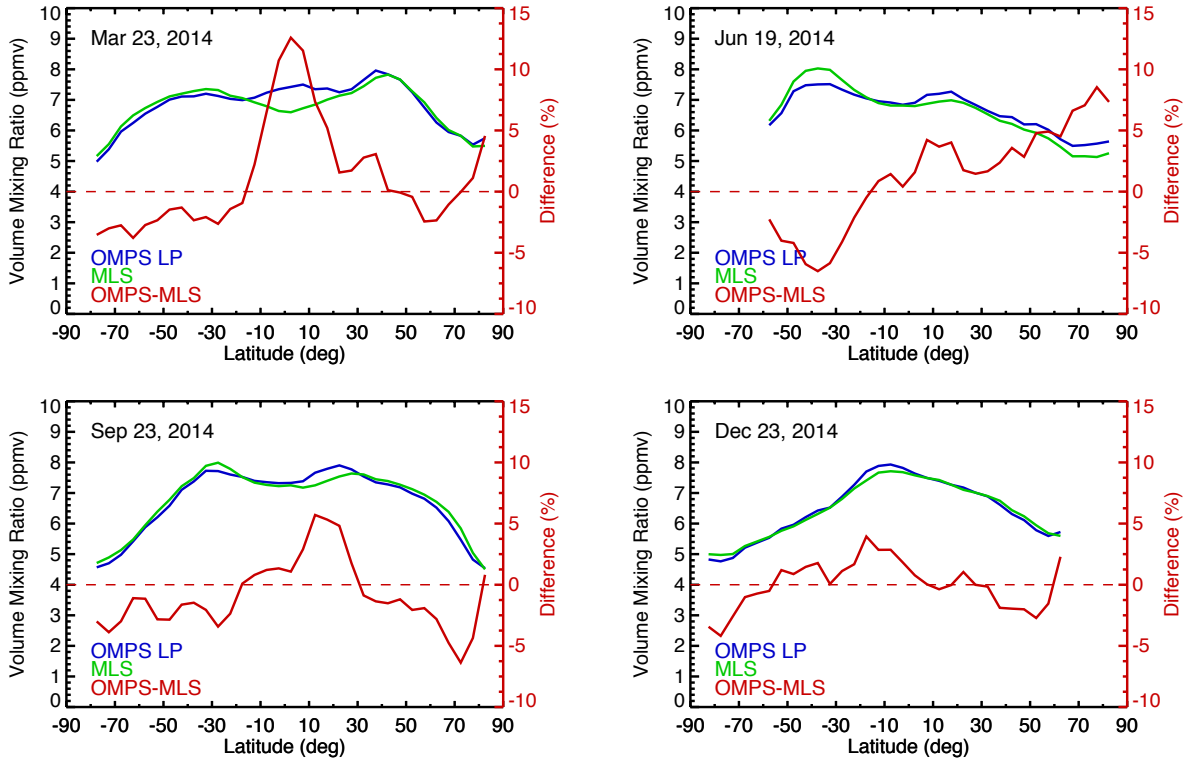

Figure 13: Daily five degree zonal means of ozone from MLS (blue), GMAO (green), and the MLS-GMAO differences (red) at 3 hPa GPH for four cardinal days. The differences are generally within 6% which if completely attributed to TH error would be ~200 m.

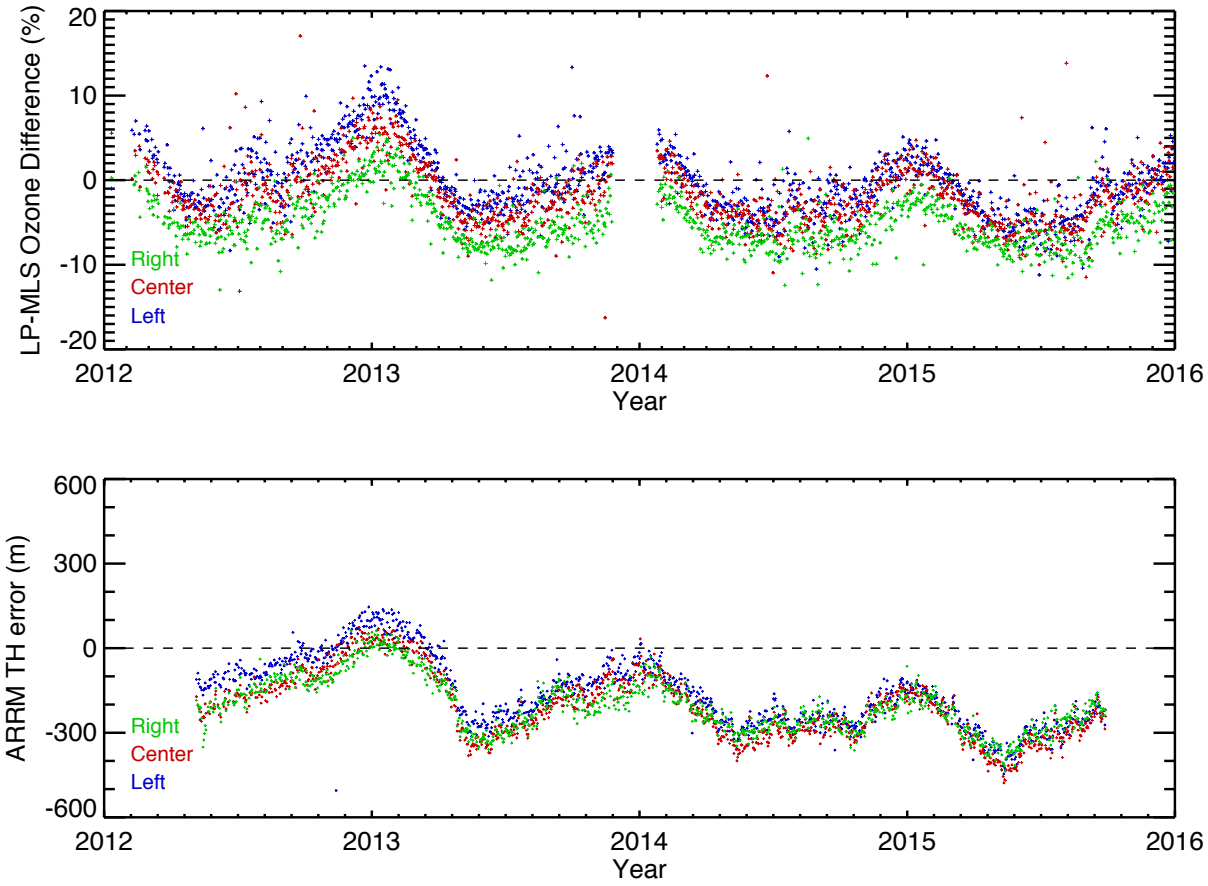

Figure 14: The time series of daily zonal mean ozone differences (%) between OMPS LP and Aura MLS for the three slits (top). OMPS LP profiles are corrected with the TH error shown in Table 1. Note the similarity in time-dependent patterns for ozone differences and TH error derived from AARM method (bottom, reprinted from Fig.9). The fact that these two completely independent methods show very similar patterns give us additional confidence in the AARM method.